Gravitational waves from the cosmological QCD transition

Germán Lugones & Victor Mourão Roque,
ABC Federal University - Brazil

STARS2013 / SMFNS2013
Havana & Varadero, CUBA, May 4-10 2013

In this work:

- relativistic hydrodynamics simulations of the cosmological quark-hadron phase transition with a lattice QCD EOS.

- We study turbulence in the primordial fluid.

- We obtain the gravitational wave signal of the fluid and compare it with the eLISA's sensitivity curve.

Reference: Mourão-Roque & Lugones, Phys. Rev. D87, 083516 (2013)

Introduction

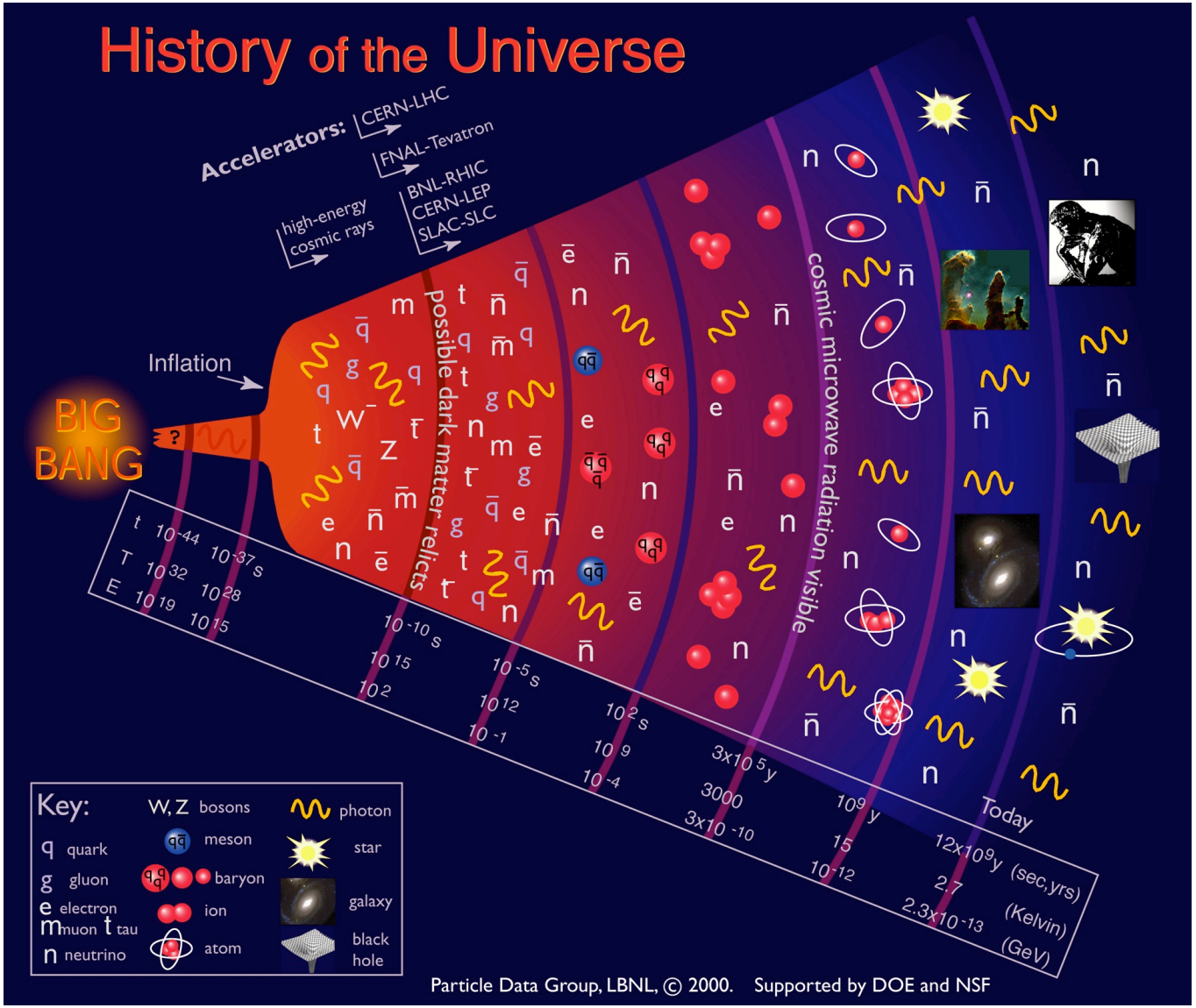

EW Phase Transition:

- electromagnetic and weak forces become differentiated
- $t_{QCD} \approx 10^{-11}$s (duration ~1μs);
- T ~ 1000 GeV

QCD Phase Transition:

- quarks confined into hadrons.
- $t_{QCD} \approx 10^{-5}$s (duration ~1μs);
- T ~ 150–200 MeV
- $d_H \approx$ 10 km (~3 ly);
- Particles: quarks (u,d,s) and gluons; leptons; photons.

Current conjectures for the QCD phase diagram. S. Gupta et al., Science **332**, 1525 (2011).

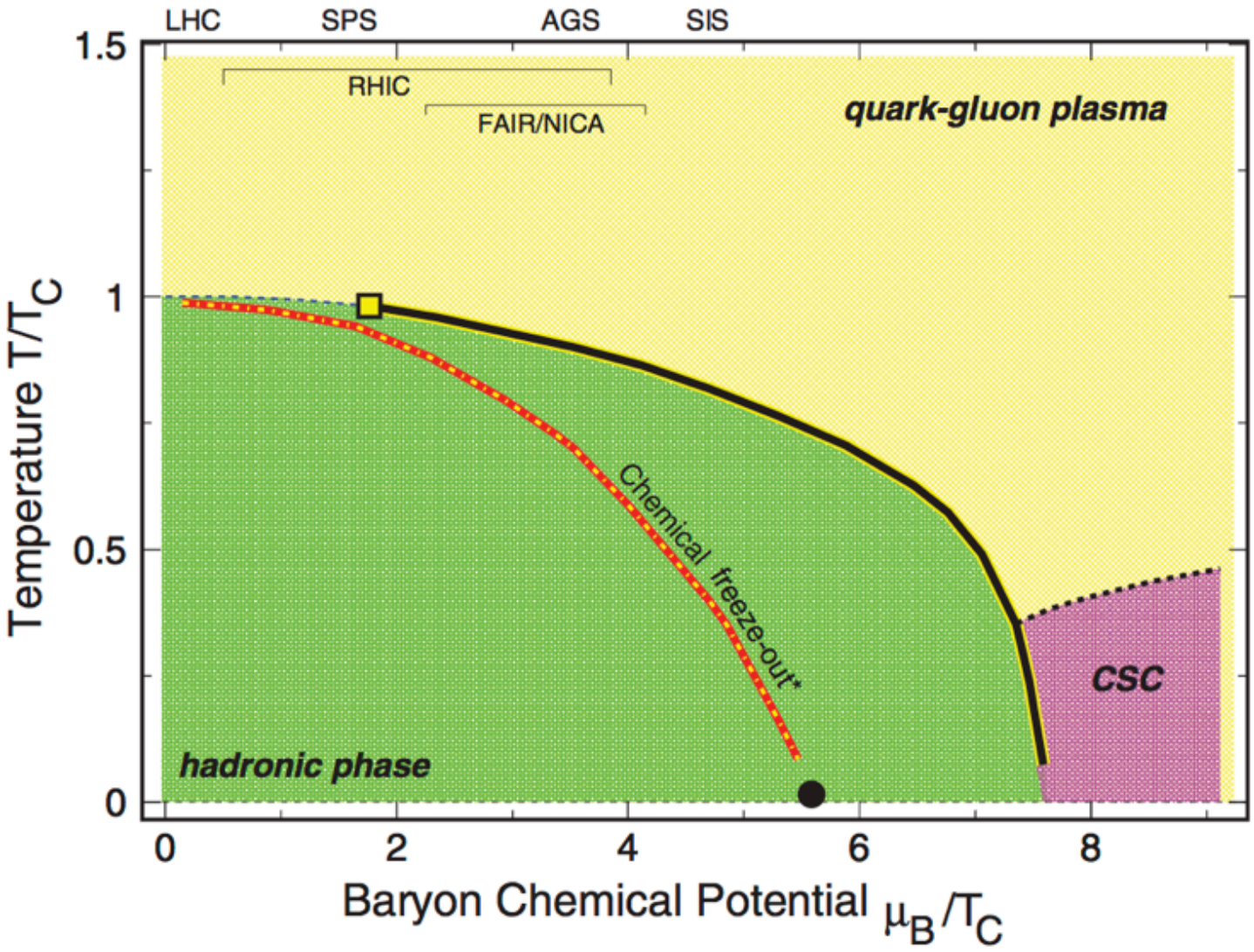

Previous Works on cosmic phase transitions:

First works: focused on the effects of a **first order** QCD transition: studies about the nucleation, growth and collision of bubbles and their relation to the generation of gravitational waves (Witten 1984, Turner & Wilczek 1990, Kosowsky &Turner 1993, Kamionkowski et al. 1994, Miller & Rezzolla 1995, etc.)

Recent works: several works on primordial turbulence, most of them focusing on a first order EW or QCD phase transition:

- Caprini, Durrer & Siemens, 2010, *Detection of gravitational waves from the QCD phase transition with pulsar timing arrays.*
- Kahniashvili, Kosowsky, Gogoberidze & Maravin, 2008, *Detectability of gravitational waves from phase transitions.*
- Kahniashvili, Brandenburg, Tevzadze & Ratra, 2010, *Numerical simulations of the decay of primordial magnetic turbulence.*
- Binetruy et al 2012, *Cosmological Backgrounds of Gravitational Waves and eLISA/NGO: Phase Transitions, Cosmic Strings and Other Sources.*

HOWEVER ! Lattice QCD results indicate that for two light (u and d) quarks and one heavy (s) quark **the transition is a crossover** (quarks are confined in hadrons in a smooth way)

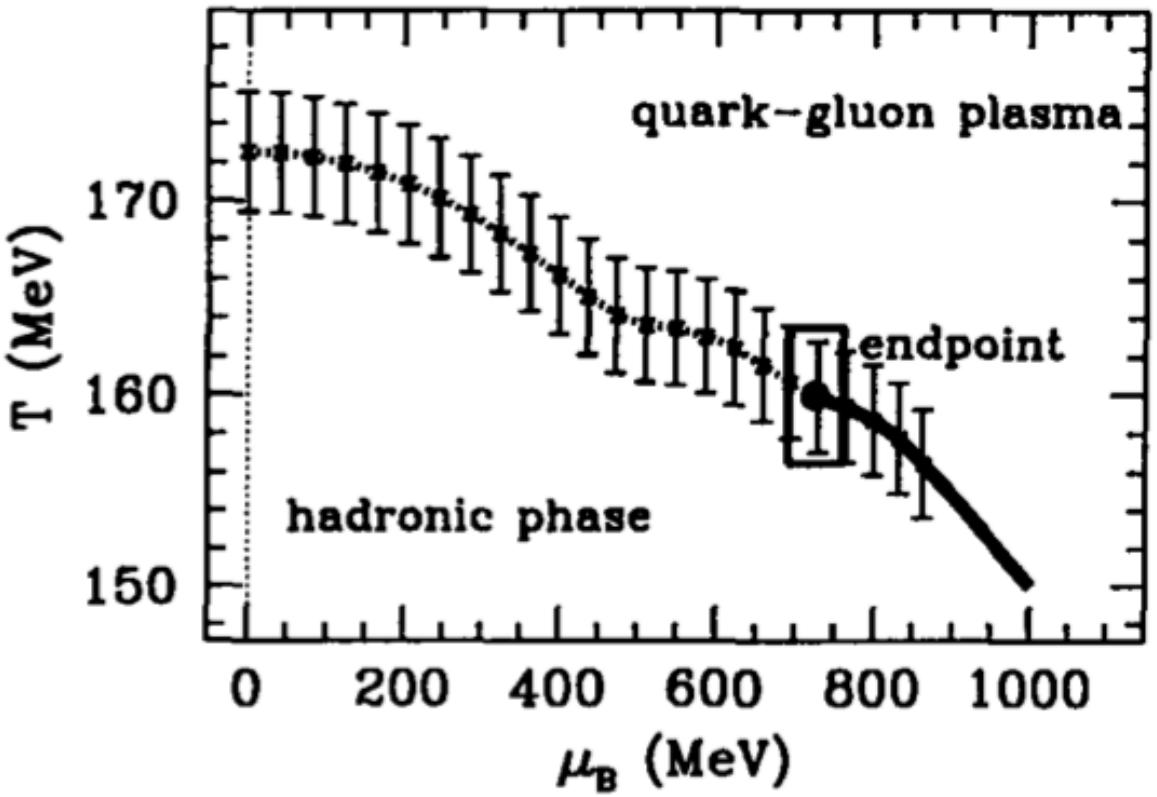

Z. Fodor,
Nuclear Physics A **715**,
319c (2003).

eLISA gravitational wave observatory:

Project for the European New Gravitational Wave Observatory (NGO) mission (derived from the previous LISA proposal, informal name “eLISA”)

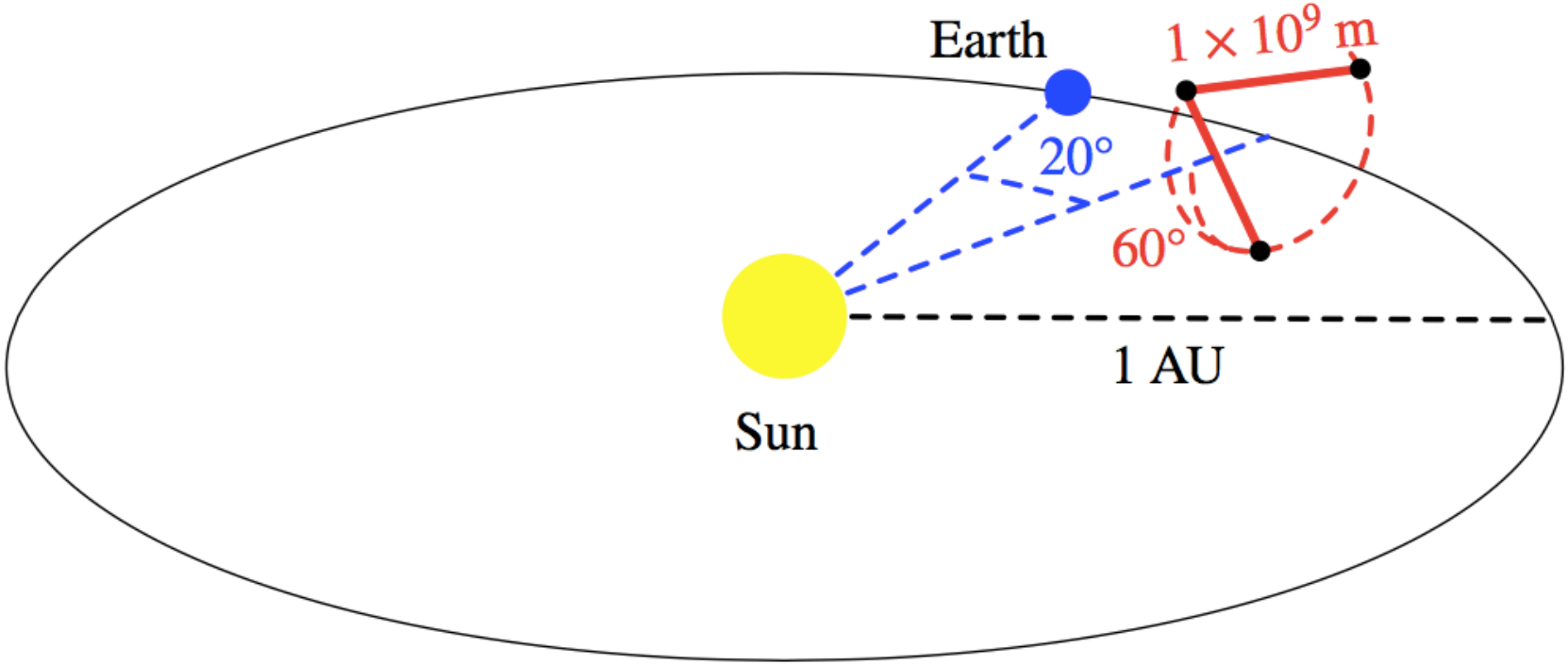

P. Amaro-Seoane et al., arXiv **astro-ph.CO**, 3621 (2012),

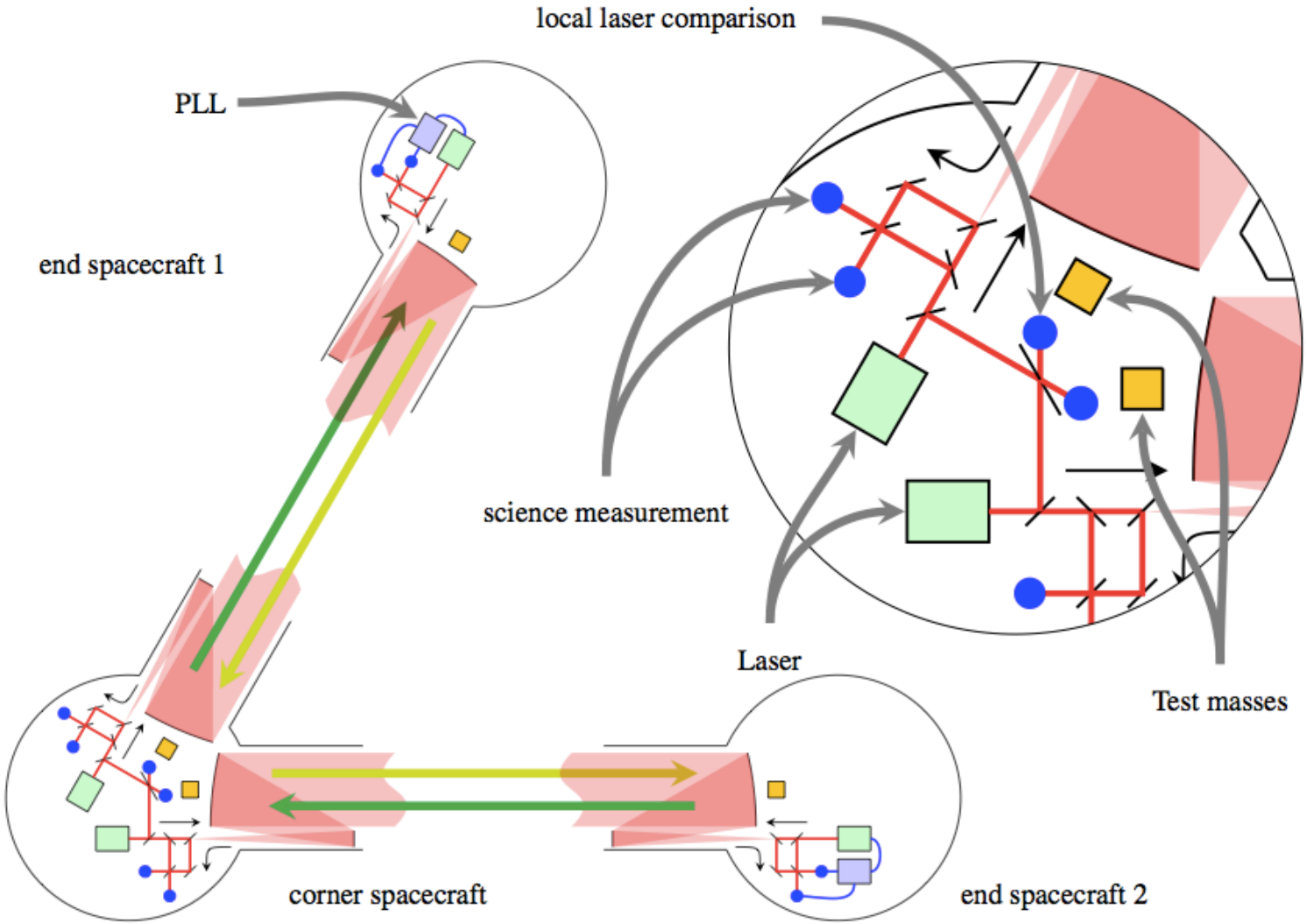

eLISA is composed by three spacecraft. The central spacecraft has two send/ receive laser ranging terminals, while the end spacecraft has one each.

P. Amaro-Seoane et al., arXiv **astro-ph.CO**, 3621 (2012).

eLISA: will survey for the first time the low-frequency gravitational wave band (about 0.1 mHz to 1 Hz)

- ✧ coalescences of massive black holes binaries;
- ✧ mergers of earlier, less-massive black holes during the epoch of hierarchical galaxy and black-hole growth;
- ✧ stellar-mass black holes and compact stars in orbits just skimming the horizons of massive black holes in galactic nuclei of the present era;
- ✧ extremely compact white dwarf binaries in our Galaxy,
- ✧ Early Universe: relics of inflation and of cosmic phase transitions.

P. Amaro-Seoane et al., arXiv **astro-ph.CO**, 3621 (2012),

Our model :

- EoS
- hydrodynamic equations
- numerical method

Lattice QCD equation of state:

- ✓ We construct the EoS using data of the Budapest-Wuppertal Collaboration with $N_f = 2 + 1$, i.e. two light (up and down) quarks and one heavy (strange) quark (Borsanyi et al. JHEP 2010)

- ✓ we add the contribution of a gas of noninteracting neutrinos, muons, electrons, photons and their antiparticles.

$T[MeV]$	p/T^4	I/T^4	c_s^2
100	0,22 (4)	0,43 (17)	0,19 (9)
115	0,29 (6)	0,56 (31)	0,18 (5)
129	0,37 (6)	0,93 (19)	0,14 (4)
139	0,46 (6)	1,46 (29)	0,13 (2)
147	0,55 (7)	1,99 (42)	0,12 (2)
152	0,63 (7)	2,47 (25)	0,12 (2)
158	0,73 (7)	2,98 (16)	0,14 (3)
166	0,89 (7)	3,43 (23)	0,16 (2)
175	1,08 (6)	3,79 (16)	0,18 (2)
200	1,61 (6)	4,03 (22)	0,22 (1)
228	2,11 (7)	3,62 (14)	0,26 (1)
250	2,43 (7)	3,20 (14)	0,27 (2)
299	2,94 (7)	2,57 (24)	0,29 (2)
366	3,38 (8)	1,80 (16)	0,32 (3)
500	3,76 (5)	1,08 (4)	0,32 (0)
600	3,93 (5)	0,80 (6)	0,32 (0)
800	4,12 (6)	0,51 (5)	0,32 (0)
1000	4,23 (6)	0,43 (11)	0,32 (0)

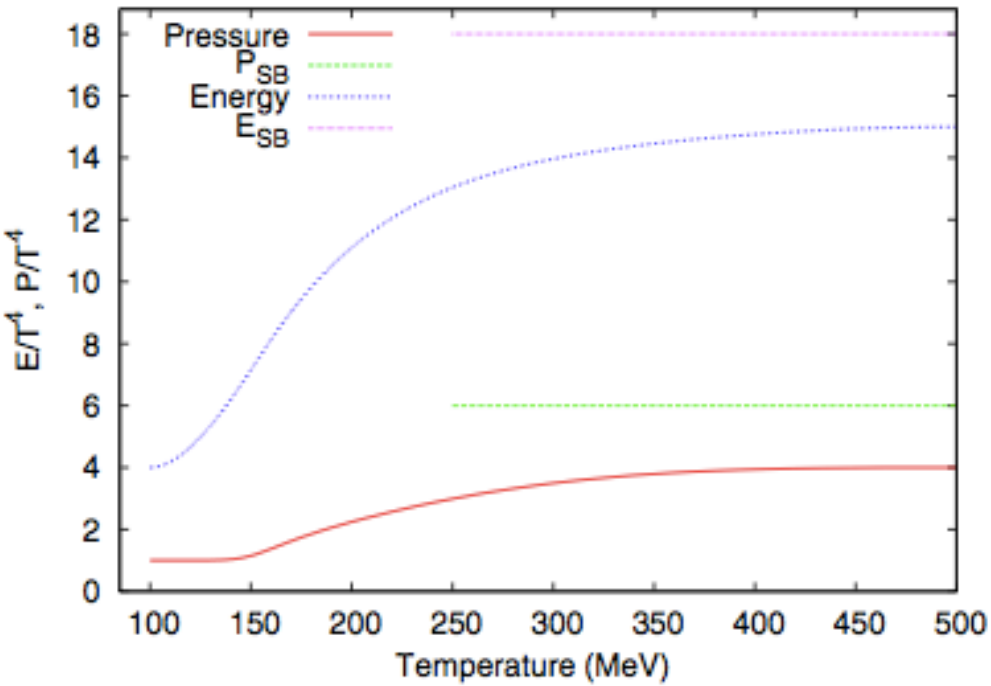

Hydrodynamics

To investigate the dynamics and evolution of the primordial fluid, we should solve the equations of hydrodynamics in the context of general relativity. However, as in previous work [28] we shall assume a flat space metric filled with a perfect fluid whose stress-energy tensor is defined by

$$T^{\mu\nu} = \rho h u^{\mu} u^{\nu} + p\eta^{\mu\nu}, \tag{1}$$

where p is the pressure, h is the specific enthalpy defined as $h = 1 + \epsilon + \frac{p}{\rho}$, ϵ is the specific internal energy and ρ is the mass density in the rest frame.

In the one-dimensional case adopted here, the hydrodynamic equations written in covariant form consist of three local conservation laws for the above stress-energy tensor $T^{\mu\nu}$ and the baryon density flow $J^{\mu} = \rho u^{\mu}$:

$$\nabla_{\mu} T^{\mu\nu} = 0, \qquad \nabla_{\mu} J^{\mu} = 0, \tag{2}$$

where we used units in which the speed of light is $c = 1$. The system must be complemented with an equation of state having the functional form $p = p(\rho, \epsilon)$.

Numerical Approach

The hydrodynamic equations presented in Eq. (2) can be recast as a hyperbolic system of first order, flux-conservative equations of the form [29]

$$\frac{\partial \mathcal{U}(\mathbf{w})}{\partial x^0} + \frac{\partial \mathcal{F}^{\mathbf{i}}(\mathbf{w})}{\partial x^i} = 0, \tag{3}$$

where in the laboratory frame the *state vector* $\mathcal{U}$ contains the *conserved* variables (D, S_i, τ) written in terms of *primitive* variables $\mathbf{w} = (\rho, v_i, p)$

$$\mathcal{U}(\mathbf{w}) = \begin{bmatrix} D \\ S_j \\ \tau \end{bmatrix} = \begin{bmatrix} W\rho \\ \rho h W^2 v_j \\ \rho h W^2 - p - W\rho \end{bmatrix}, \tag{4}$$

and the *flux vector* $\mathcal{F}^{\mathbf{i}}(\mathbf{w})$ is given by

$$\mathcal{F}^{\mathbf{i}}(\mathbf{w}) = \begin{bmatrix} D v^i \\ S_j v^i + p\delta^i_j \\ \tau v^i + p v^i \end{bmatrix}, \tag{5}$$

with $W = (1 - v^i v^j)^{-1/2}$ being the Lorentz factor.

Numerical details:

- **the code:**
  - based on the Godunov Method with the Riemann Solver of Roe.
  - we use a *monotone upstream centered scheme for conservation laws* (MUSCL), with a standard "minmod" sloper limit for the reconstruction of the cell centered quantities before the computation of the numerical fluxes.
  - integration in time is performed by using a third order strong-stability-preserving Runge-Kutta scheme with five stages.

- We consider a computational domain with a length of 100 m, with 16.384 spatial cells (2^{14}) and evolve the system for times larger than 1 μs.

Turbulence

- ✓ Since we are considering a **crossover transition**, we do not expect large perturbations near T_c as would be the case for a first order transition.

- ✓ Thus, we assume that fluctuations present at the QCD epoch were generated by some event in the previous history of the Universe, e.g. at the electroweak scale or at an even smaller scale related to inflation, cosmic strings, etc.

- ✓ These fluctuations are conjectured to survive until the beginning of the QCD phase transition due to the extremely low viscosity of the primordial fluid:

  - Experimental results (Song et al 2011, Heinz et al. 2012): viscosity of the QGP at LHC and RHIC is extremely small (but μ is not strictly zero as in the early Universe).
  - Theoretical calculations (Ahonen 1998): at μ =0 viscosity is small even with the inclusion of leptons and photons.

- ✓ According to the theory of turbulence, larger eddies break down to smaller ones, i.e. there is a ***cascade of kinetic energy from large to small scales***. This cascade stops at a small damping length scale l_D determined by the viscosity of the fluid.

- ✓ In models of ***1st order transitions*** there is a continuous injection of energy (bubble collisions) and viscous dissipation at small scales → this leads to the well known Kolmogorov spectrum ($\sim k^{-2/3}$ or variations of this, negative slope!) [e.g. Kosowsky et al. 2002, Gogoberidze et al. 2007, Caprini 2010, etc.]

- ✓ For a ***crossover transition***, there isn't a continuous injection of energy. Since the viscosity is tiny, cascading accumulates energy at the small scales (we expect a turbulent spectrum with a positive slope)

Since the size of possible disturbances at the time of the transition is unknown we have considered three different kinds of random initial profiles:

(a) random temperature inhomogeneities in a fluid at rest,
(b) random velocity fluctuations within a fluid with an initial uniform temperature, and
(c) random temperature and velocity fluctuations.

The maximum amplitudes are:

- ✓ $\Delta T/T_c = 10^{-2}, 10^{-3}, 10^{-4}$ around $T_c = 170$ MeV and/or
- ✓ $\Delta v/c = 10^{-1}, 10^{-2}, 10^{-3}$

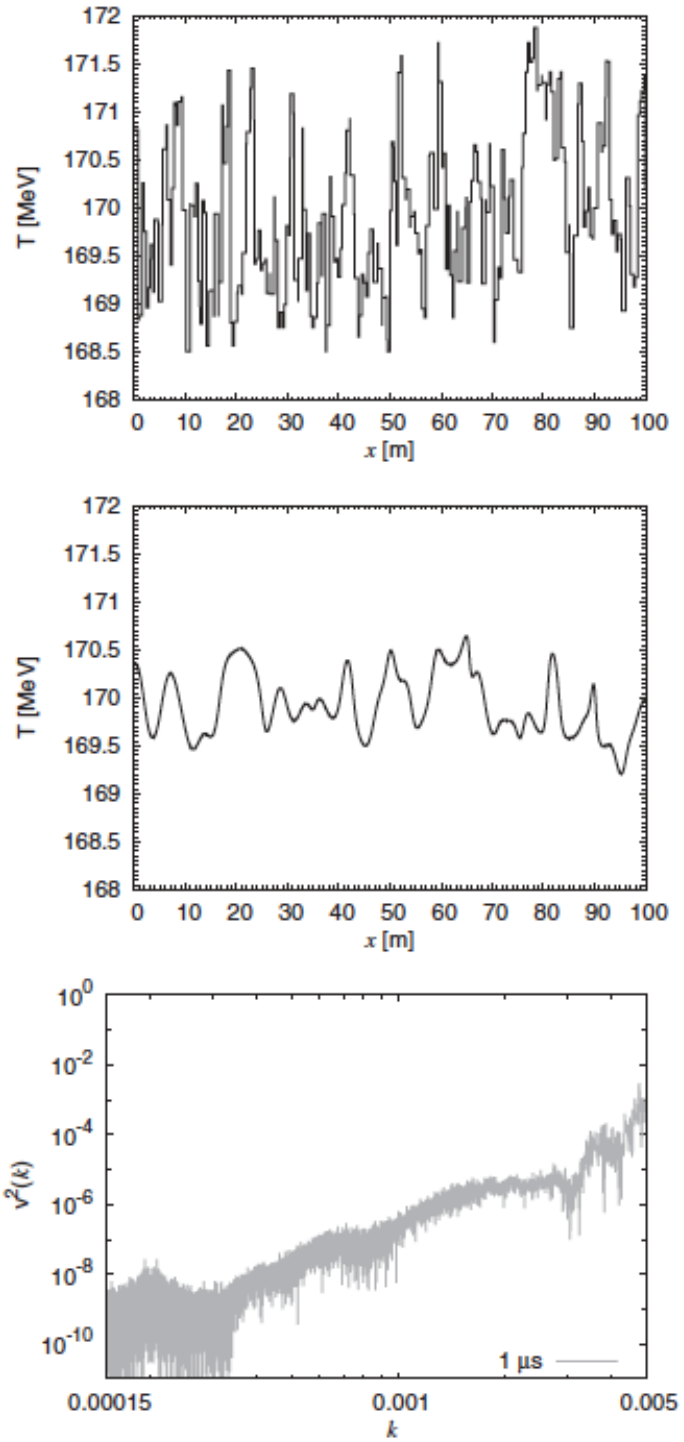

FIG. 2. Top: Initial temperature profile with random temperature fluctuations of maximum amplitude $(\Delta T)/T_c = 10^{-2}$. The fluid is considered at rest at $t = 0$. Center: Temperature profile after 1 μs of evolution. Temperature inhomogeneities are smoothed and the fluid develops a turbulent motion. Bottom: Velocity spectrum $\langle v^2(k)\rangle$ of the turbulent motion of the fluid at $t = 1$ μs. There is an energy cascading from the larger to the smaller scales. Energy is not dissipated at the smallest scale because of the negligible viscosity of the primordial fluid. We have considered several different random initial conditions for the temperature profile, all with maximum amplitude $(\Delta T)/T_c = 10^{-2}$. All of them present the same behavior as presented in this figure.

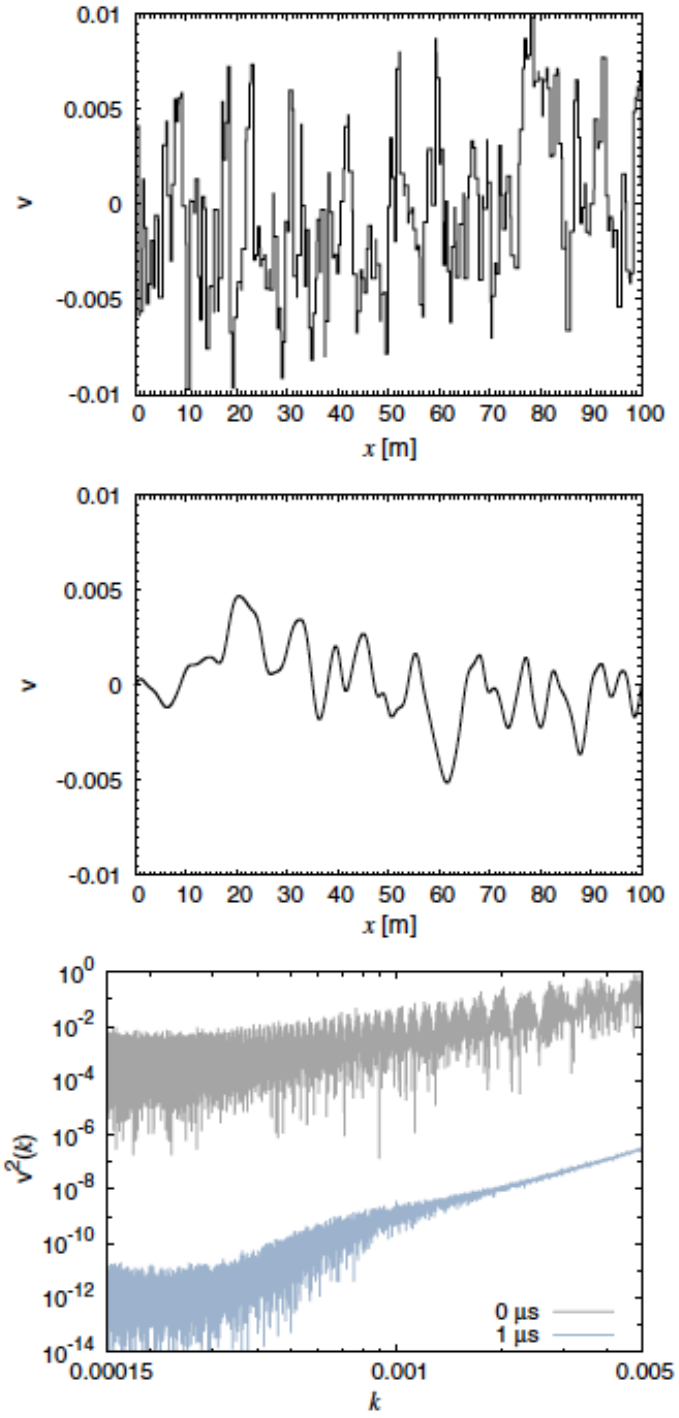

FIG. 4 (color online). Top: Initial velocity profile with random velocity fluctuations of maximum amplitude $(\Delta v)/c = 10^{-2}$ and constant temperature $T = T_c \equiv 170$ MeV. Center: Velocity profile after 1 μs of evolution. Bottom: Velocity spectrum $\langle v^2(k)\rangle$ at $t = 0$ and $t = 1$ μs. The final spectrum is steeper due to the energy cascading from the large to the small scales.

In a crossover transition, the velocity spectrum is very different from the Kolmogorov power law considered in most studies of first order transitions.

Gravitational Waves

Gravitational Waves

For each hydrodynamic simulation, we store the stress-energy tensor $T^{\mu\nu}(x,t)$ at all time-steps.

We obtain $T^{\mu\nu}(k,\omega)$ by a fast Fourier transform (FFT)

Using the Weinberg formalism, in the weak-field approximation, the total energy radiated in gravity waves is

$$\frac{dE}{d\Omega} = 2G\Lambda_{ij,lm}(\hat{\boldsymbol{k}}) \int_0^\infty \omega^2 T^{ij*}(\boldsymbol{k},\omega) T^{lm}(\boldsymbol{k},\omega) d\omega,$$

where $\Lambda_{ij,lm}$ is the projection tensor:

$$\Lambda_{ij,lm}(\hat{\boldsymbol{k}}) = \delta_{il}\delta_{jm} - 2\hat{\boldsymbol{k}}_j\hat{\boldsymbol{k}}_m\delta_{il} + \frac{1}{2}\hat{\boldsymbol{k}}_i\hat{\boldsymbol{k}}_j\hat{\boldsymbol{k}}_l\hat{\boldsymbol{k}}_m - \frac{1}{2}\delta_{ij}\delta_{lm}$$
$$+ \frac{1}{2}\delta_{ij}\hat{\boldsymbol{k}}_l\hat{\boldsymbol{k}}_m + \frac{1}{2}\delta_{lm}\hat{\boldsymbol{k}}_i\hat{\boldsymbol{k}}_j,$$

Our model is axially symmetric about the z axis, thus, without loss of generality, we can take:

$$\hat{\boldsymbol{k}}_x = \sin\theta, \qquad \hat{\boldsymbol{k}}_y = 0, \qquad \hat{\boldsymbol{k}}_z = \cos\theta.$$

Therefore, the projector tensor reads

$$\Lambda_{ij,lm} = \Lambda_{lm,ij},$$
$$\Lambda_{ij,lm}\delta_{ij} = 0,$$
$$\Lambda_{ij,lm}\hat{k}_i\hat{k}_j = 0,$$
$$\Lambda_{ij,lm}\delta_{iz}\delta_{jz}\delta_{lz}\delta_{mz} = \Lambda_{zz,zz} = \frac{1}{2}(1-\hat{k}_z^2)^2 = \frac{1}{2}\sin^4\theta.$$

Thus, the total energy per unit frequency interval

$$\frac{dE}{d\omega} = G\omega^2 \int |T^{zz}(\boldsymbol{k},\omega)\sin^2\theta + T^{xx}(\boldsymbol{k},\omega)\cos^2\theta - T^{yy}(\boldsymbol{k},\omega)|^2 d\Omega,$$

$$T^{zz}(\boldsymbol{x},t) = h\rho v_z^2 - p,$$
$$T^{xx}(\boldsymbol{x},t) = T^{yy}(\boldsymbol{x},t) = p.$$

FFT

$T^{zz}(\boldsymbol{k},\omega)$, $T^{xx}(\boldsymbol{k},\omega)$ and $T^{yy}(\boldsymbol{k},\omega)$

Finally, integrating over angles:

$$\frac{dE}{d\omega} = \frac{32\pi}{15} G\omega^2 |T^{zz}(\boldsymbol{k},\omega) - T^{xx}(\boldsymbol{k},\omega)|^2.$$

Present spectrum

In order to compare our results with eLISA/NGO, we describe the spectrum in terms of a characteristic amplitude of the stochastic background defined as [40]

$$h_c(f) \equiv 1.3 \times 10^{-18} [\Omega_{GW}(f) h_0^2]^{1/2} \left(\frac{1 \text{ Hz}}{f} \right), \qquad (23)$$

where $f = \omega/(2\pi)$, $h_0 \equiv H_0/(100 \text{ kms}^{-1} \text{ Mpc}^{-1})$ with H_0 as the Hubble constant, and Ω_{GW} is the energy density of the gravitational waves,

$$\Omega_{GW} = \frac{1}{\rho_c} \left(f \frac{dE}{df} \right), \qquad (24)$$

$\rho_c = 3H_0^2/8\pi G$ being the critical density. Finally, we have to consider the redshift suffered by the waves in their way to the present Universe [40]:

$$f_0 = 8 \times 10^{-14} f_* \left(\frac{100}{g_*} \right)^{1/3} \left(\frac{1 \text{ GeV}}{T_*} \right) \text{ Hz}, \qquad (25)$$

$$\Omega_{GW} = 1.67 \times 10^{-5} h_0^{-2} \left(\frac{100}{g_*} \right)^{1/3} \Omega_{GW*}, \qquad (26)$$

where the subscript 0 corresponds to present values and the subscript $*$ to the values at the epoch of the transition.

e.g. M. Maggiore, Phys. Rep. **331**, 283 (1999).

Random fluctuations of maximum amplitude:

- ✓ $\Delta T/T_c = 10^{-2}, 10^{-3}, 10^{-4}$ around $T_c = 170$ MeV and/or
- ✓ $\Delta v/c = 10^{-1}, 10^{-2}, 10^{-3}$

Our goal is to determine the smallest fluctuation amplitude that would be detected by eLISA, considering the motion of the fluid induced by the initial condition as a source of gravitational radiation.

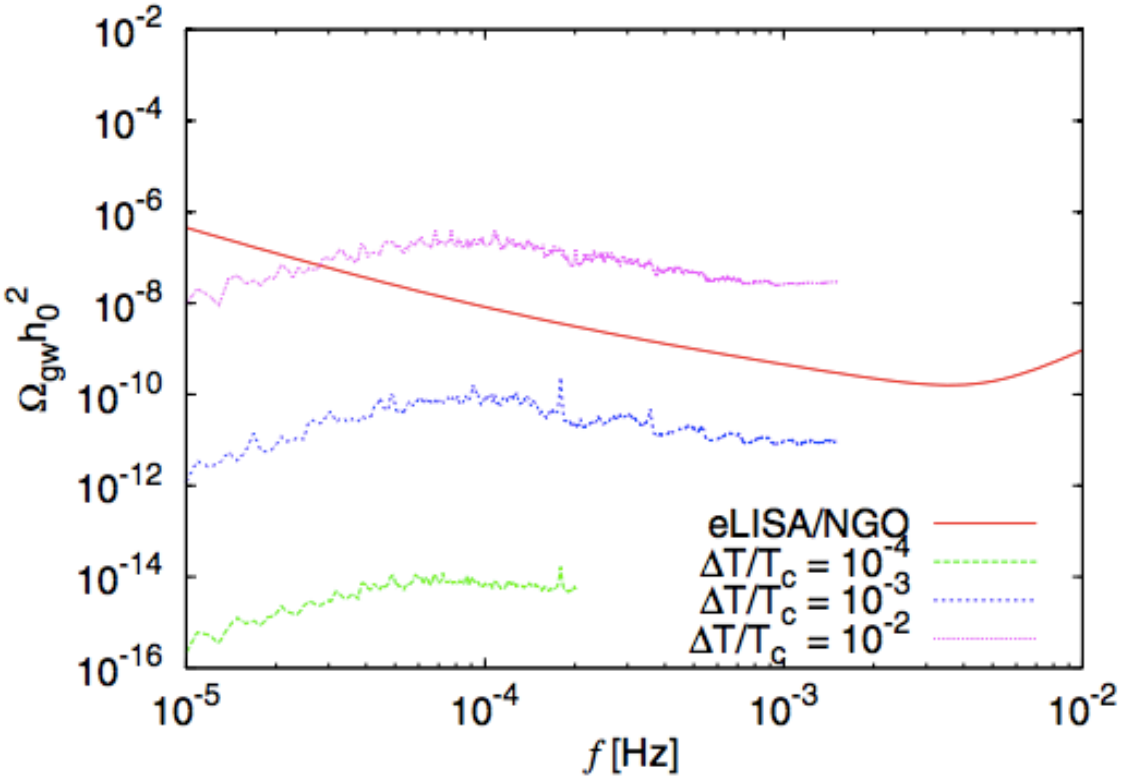

FIG. 3 (color online). Spectra of gravitational waves for hydrodynamic simulations with different initial conditions at the beginning of the QCD epoch. We considered random temperature fluctuations of maximum amplitude $(\Delta T)/T_c = 10^{-2}$ (see Fig. 2) as well as 10^{-3} and 10^{-4}. For comparison we show the sensitivity curve of eLISA/NGO computed using the expected instrumental noise and the confusion noise generated by unresolved galactic binaries [26].

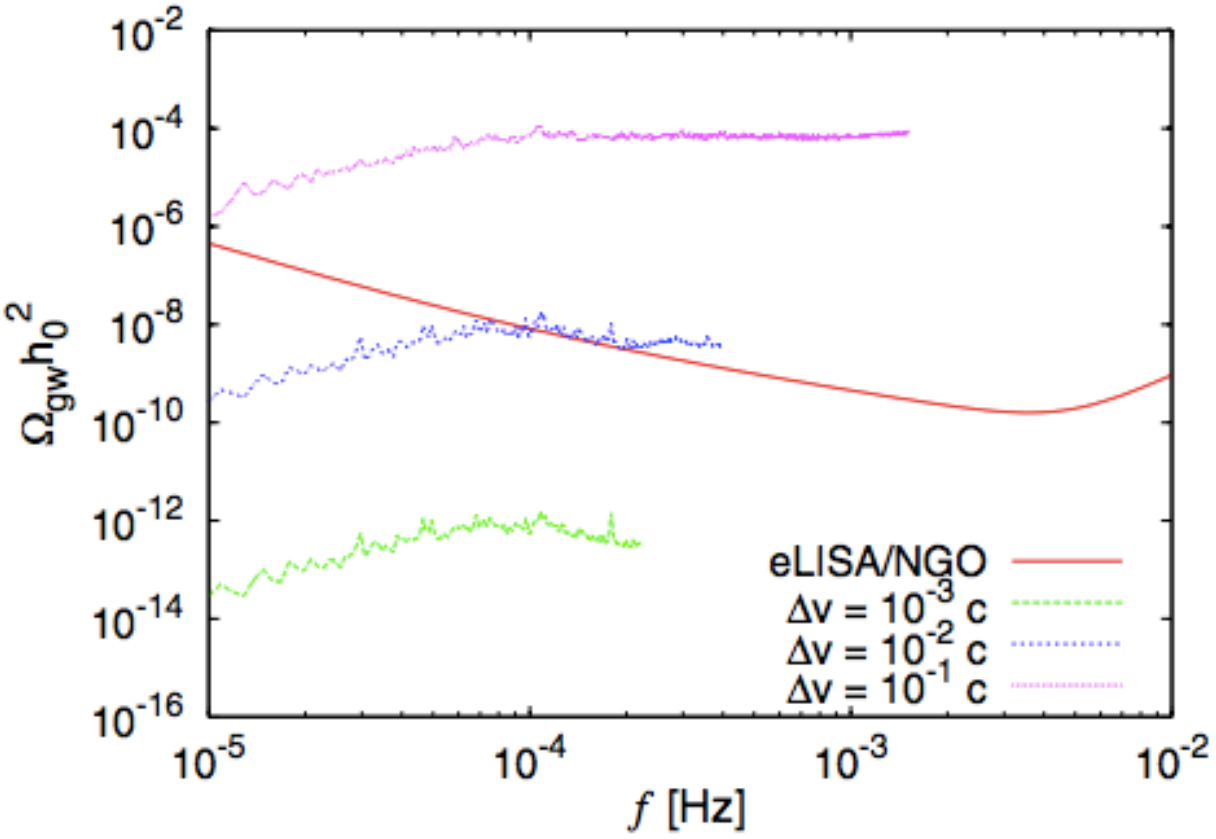

FIG. 5 (color online). Spectrum of gravitational waves for simulations with initial random velocities $(\Delta v)/c = 10^{-3}, 10^{-2}, 10^{-1}$.

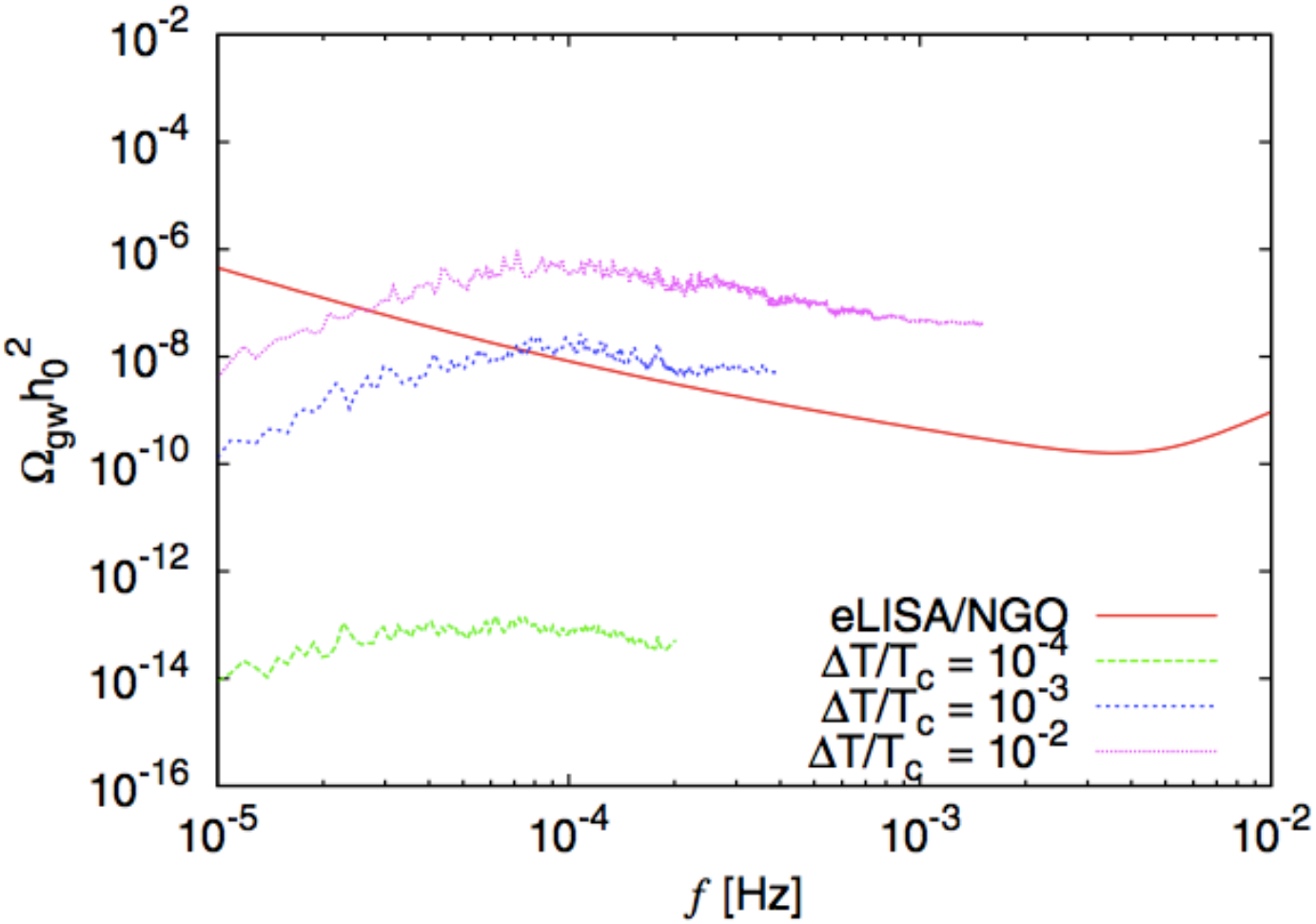

FIG. 8 (color online). Spectrum of gravitational waves for $(\Delta v)/c = 10^{-2}$ and different initial temperature fluctuations.

Conclusions

CONCLUSIONS:

- ✓ **TURBULENCE**: our results show that **the velocity spectrum is very different from the Kolmogorov power law considered in most studies** of primordial turbulence that focus on first order transitions. This is due to the fact that there is no continuous injection of energy into the system and the viscosity of the fluid is negligible. Thus, as kinetic energy cascades from the larger to the smaller scales, a large amount of kinetic energy is accumulated at the smallest scales due to the lack of dissipation.

- ✓ **GRAVITATIONAL WAVES**: We have obtained the spectrum of the gravitational radiation emitted by the motion of the fluid for different initial profiles that include random T and v fluctuations of different maximum amplitudes. **We find that if typical fluctuations have an amplitude $\Delta v/c \geq 10^{-2}$ and/or $T/\Delta T_c \geq 3 \times 10^{-3}$, they would be detected by eLISA at frequencies larger than $\approx 10^{-4}$ Hz.**

STARS2013 / SMFNS2013

Havana & Varadero, CUBA, May 4-10 2013